ELSEVIER

Journal of Power Sources 53 (1995) 207–214

JOURNAL OF POWER SOURCES

Wrought lead–calcium–tin alloys for tubular lead/acid battery grids

R. David Prengaman

Research & Development, RSR Corporation, 1111 W. Mockingbird Lane, Dallas, TX 75247, USA

Received 22 September 1994

Abstract

Lead/acid batteries with tubular grids for the positive electrodes give flatter discharge curves and higher cycle life than batteries using flat plates. Most tubular grids for motive-power batteries contain 9–11 wt.% antimony. Recently, alloys with 1–6 wt.% antimony have been used for reduced maintenance batteries. Sealed, valve-regulated batteries with tubular positive grids for motive power, telecommunications, and UPS service are produced from cast lead–calcium–tin alloys. While these alloys permit the construction of such batteries, cast Pb–Ca–Sn alloys are significantly inferior to cast Pb–Sb alloys in mechanical properties. Wrought Pb–Ca–Sn alloys, when used for tubular grids, permit the application of maintenance-free alloys with mechanical properties comparable with, or higher than, those of high-antimony alloys. Wrought materials increase life due to the absence of casting defects. Wrought lead–calcium alloys also offer a dramatic improvement in creep and corrosion resistance compared with conventional cast, tubular, Pb–Ca–Sn alloys, as well as superior conductivity to cast Pb–Sb. Wrought Pb–Ca–Sn alloys permit the production of tubular grids at high speed in shapes and forms that are difficult to produce from cast materials. These grid shapes can lead to higher performance, higher discharge-rate, tubular plates. This paper discusses the mechanical properties, grain structure, and corrosion behaviour of cast and wrought Pb–Ca–Sn and Pb–Sb alloys for tubular grids. It also suggests manufacturing techniques for high performance, wrought, tubular plates.

Keywords: Lead/acid batteries; Grids; Lead–calcium–tin alloys

1. Background

Lead/acid batteries with tubular positive grids have been used extensively throughout the world for traction applications [1,2]. These grids have traditionally employed lead–antimony alloys of 9–12 wt.% Sb. These batteries have shown excellent rechargeability, long life, and relatively stable discharge curves with time. The high-antimony alloys offer excellent fluidity, uniform grain structure, high initial and aged mechanical properties for ease in processing, and uniform (although relatively high) corrosion rates.

The major problem in the use of high-antimony alloys is the transfer of antimony from the positive to the negative plate during cycling. Antimony reduces the hydrogen evaluation voltage and leads to the generation of hydrogen gas and water loss during charging. To produce lower-maintenance batteries, the antimony content of the tubular grids has been reduced to 2–6 wt.%. These alloys have lower mechanical properties and are more difficult to process than the traditional high-antimony alloys.

Tubular, gel, valve-regulated lead/acid (VRLA) batteries using cast positive grid alloys of lead–calcium or lead–calcium–tin have been developed for telecommunications and traction service. Positive Pb–Ca–(Sn) grids produce significantly reduced water loss when compared with Pb–Sb alloys. The grids produced from Pb–Ca alloys, however, generally suffer from reduced cycle life. In addition, tubular Pb–Ca positive grids suffer from growth and active-material shedding. In general, tubular positive plates using Pb–Ca–(Sn) alloys have reduced energy density and a lower rate of discharge than Pb–Sb alloy grids. It is believed that the cast Pb–Ca–(Sn) alloys utilized in VRLA tubular grids have insufficient mechanical properties, a grain structure conducive to corrosion, and a chemical composition optimized for processing rather than for ultimate cycling performance.

Wrought Pb–Ca–(Sn) alloys offer superior mechanical properties, contain uniform grain structures for reduced

SSDI 0378-7753(94)01975-2

corrosion, and permit the use of optimized chemical composition. The alloys, however, are in solid form. New processes for fabricating tubular grids from wrought metals must be utilized for VRLA batteries. The new processes may lead to a new generation of tubular VRLA batteries.

2. Lead–antimony alloys

Cast lead–antimony alloys, particularly the high (9–12 wt.% Sb) antimony alloys are strengthened by a eutectic phase that is comprised of alternating plates of antimony and lead. The high-antimony alloys consist primarily of the eutectic phase. Fig. 1 shows the grain structure of a 10 wt.% Sb cast alloy. The antimony platelets are significantly harder and stronger than the lead phase contained between them. Because the antimony plates do not deform as antimony content is increased, the ultimate tensile strength, yield strength, and creep resistance also increase. The rigidity of the platelets also reduces the elongation of the material. The high yield strength, high creep strength, and low elongation permit grids produced from these alloys to resist deformation by the stresses induced by the charge–discharge reactions of the active material during cycling. Table 1 shows the mechanical properties of various Pb–Sb alloys. The mechanical properties decrease markedly below 6 wt.% Sb, as would be expected because of the lower level of eutectic in the alloy at low antimony contents. The most significant property change with variation in antimony content is creep resistance as measured by the stress rupture test (i.e., time to failure at a given stress level). There is a three orders of magnitude difference between the low- and high-antimony alloys.

Virtually all lead antimony alloys are used in the as-cast form and for good reason. Table 1 also shows the mechanical properties of some wrought Pb–Sb alloys. While the ultimate tensile stress (UTS), yield strength (YS) and elongation time (EL) are reduced, the creep resistance is particularly affected. Rolling lead–antimony alloys destroy the cast-in strengthening mechanism of the eutectic phase [3]. Fig. 2 shows the grain structure of a cast 6 wt.% Sb alloy. Fig. 3 gives the grain structure of the same alloy rolled with a 10:1 reduction in thickness. The eutectic particles are broken up and turned in the direction of the rolling. In addition, and as shown in Fig. 4, the structure becomes recrystallized and this further reduces the mechanical properties. The dramatic reduction of the mechanical properties in wrought Pb–Sb alloys has virtually precluded these alloys from use in either tubular- or flat-plate batteries.

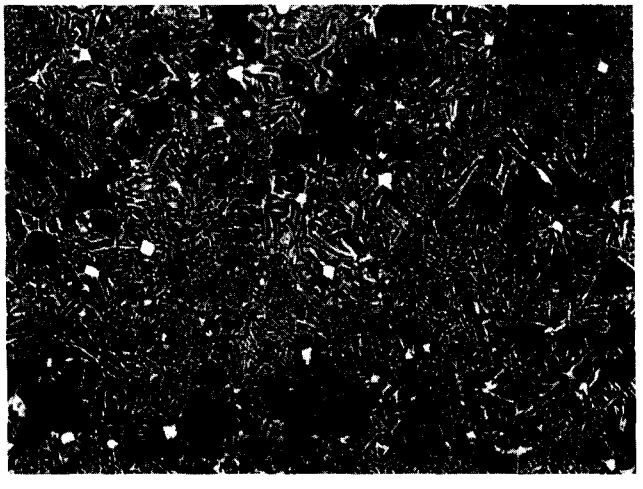

Fig. 1. Grain structure of Pb–10wt.%Sb cast alloy. Magnification 160×.

The corrosion of Pb–Sb alloys proceeds by attack of the antimony eutectic phase, as seen in Fig. 5 for a cast Pb–6wt.%Sb alloy. The attack also solubilizes some of the antimony and permits the stresses induced by the higher volume of the corrosion product to be accommodated. Thus, higher antimony alloys withstand corrosion stresses very well. Rolled Pb–Sb alloys, on the other hand, have no continuity in the eutectic particles. Fig. 6 shows the corrosive attack of a rolled Pb–6wt.%Sb alloy. In these alloys, it is primarily the lead phase, rather than the antimony eutectic phase, that is attacked because the antimony particles are isolated from one another.

3. Alloys for valve-regulated batteries

Lead–calcium alloys have been used for many years in flooded-electrolyte, reduced gassing batteries, primarily in telephone and submarine applications [4,5]. These alloys have been binary lead–calcium alloys.

3.1. Lead–calcium alloys

Cast and wrought Pb–Ca alloys are significantly inferior to cast Pb–Sb alloys, particularly in creep resistance. Table 2 shows the mechanical and corrosion properties of various cast Pb–Ca alloys. The mechanical properties peak at about 0.07 wt.% calcium and become significantly reduced as the calcium content is increased. This is just the opposite of what might be expected where additional alloying elements generally increase mechanical properties. Calcium contents above about 0.06 wt.% calcium have fine grains due to cellular precipitation of calcium as Pb_3Ca [6–8].

Like the mechanical properties, there is a dramatic increase in the rate of corrosion as the calcium content is increased. This behaviour is believed to be due to the formation of fine grains and primary Pb_3Ca particles. The same mechanism is considered to reduce the mechanical properties as the calcium content is increased.

Table 1
Mechanical properties of lead–antimony alloys

Antimony content (wt.%)	Yield strength aged (MPa)	UTS (MPa)	Ratio YS/UTS	Elongation (%)	Creep to fail at 27.6 MPa (h)
Cast					
11	74.4	75.9	0.98	5	1200 (8000) at 20.7 MPa
6	71.0	73.8	0.962	8	1000 (6000) at 20.7 MPa
3	55.2	65.5	0.843	10	630
2	37.9	46.9	0.808	15	190
1	19.3	37.9	0.509	20	3
0	3.5	11.7	0.299	55	
Rolled					at 20.7 MPa
11	23.8	36.3	0.65	35	4.5
6	19.5	30.6	0.64	35	1.5
3	16.3	24.6	0.66	40	(extrapolated values)

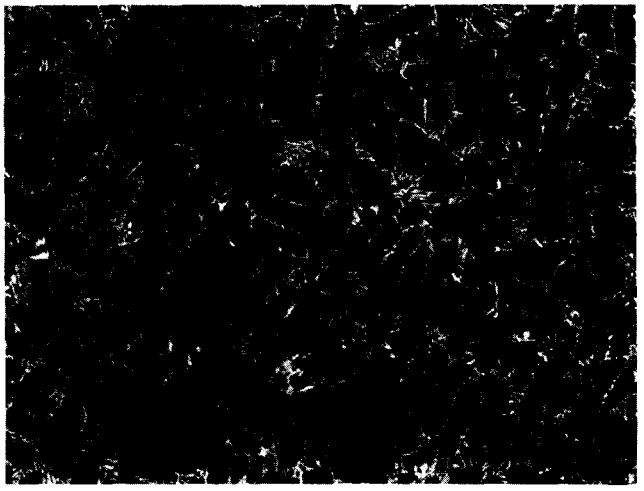

Fig. 2. Grain structure of Pb–6wt.%Sb alloy. Magnification 160×.

Fig. 3. Grain structure of wrought Pb–6wt.%Sb alloy. Magnification 120×.

Pb–Ca alloys used for positive grids of telecommunications batteries employ low contents of calcium. These alloys have a very large grain size, as shown in Fig. 7. Corrosion occurs primarily at grain boundaries. Because the corrosion is restricted to only a few areas, the grids are very thick, and the batteries are mainly used for float service and are cycled infrequently; grid growth and positive grid failure is minimal.

When the binary Pb–Ca alloys were used in VRLA batteries that employ thinner grids, higher calcium contents were used to aid processing (faster ageing rate) in both tubular and flat plate designs. These alloys produced fine grains, as seen in Fig. 8. Grid growth, corrosion, paste shedding, and premature capacity loss occurred rapidly. The creep properties of the Pb–Ca alloys are two orders of magnitude lower than the lowest Pb–Sb alloy used for tubular or flat plate cycling batteries. Tensile strength decreases as the calcium content is increased and subsequent creep rate is increased. Corrosion of Pb–Ca alloys increases as a function of the calcium content, and is particularly accelerated above 0.07 wt.% Ca where the mechanical properties begin to decline Despite the use of very low calcium alloys in some VRLA battery applications, the alloys are not appropriate for cycling service due to the rapid loss of capacity.

3.2. *Lead–calcium–tin alloys*

Tin additions to Pb–Ca alloys significantly increase the mechanical properties of cast grids. Table 3 [9] shows the mechanical and corrosion behaviour of alloys

Fig. 4. Grain structure of rolled Pb–6wt.%Sb. Magnification 640×.

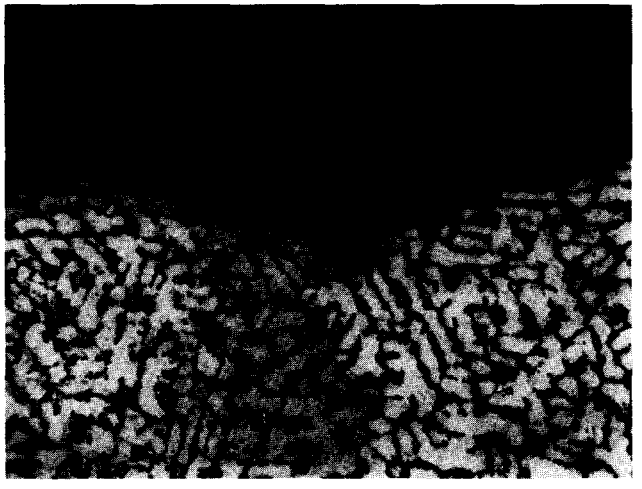

Fig. 5. Corrosion of cast Pb–6wt.%Sb alloy. Magnification 200×.

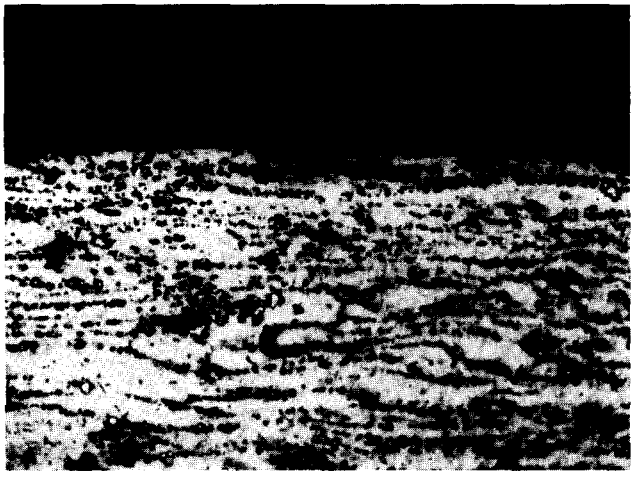

Fig. 6. Corrosion of wrought Pb–6wt.%Sb alloy. Magnification 200×.

from 0.025–0.14 wt.% Ca at 0.5 and 1.5 wt.% Sn, respectively. Tin additives to the Pb–Ca alloys increase the mechanical properties by changing the mode of precipitation from Pb_3Ca to the more stable $Pb(Sn,Ca)_3$ [10,11]. In addition, tin aids in the electrochemical properties of the alloy by preventing passivation and permitting recharge of batteries from the deeply-discharged condition [12].

Pb–Ca–Sn alloys show increasing mechanical properties as tin is increased at all calcium contents. The alloys also exhibit peak mechanical properties at about the peritectic composition. Significant decreases in yield strength and creep resistance are seen in alloys above about 0.08 wt.% Ca. In these alloys, the grain size is decreased and much of the precipitate that strengthens the material is Pb_3Ca instead of the more stable, stronger, and more effective $Pb(Sn,Ca)_3$. The most important difference in Pb–Ca–Sn alloys occurs above and below a line demarcating about a 9:1 ratio of tin content to calcium content (r). Above that ratio, the alloys are in a stable, high strength region in the fully aged condition and exhibit relatively large grain sizes and tin segregation, as seen in Fig. 9. Below $r=9{:}1$, despite high tin contents, the cellular precipitation reactions and primary Pb_3Ca particles serve to produce a very fine grain size and reduced tin segregation, as presented in Fig. 10.

In the region above $r=9{:}1$, the initial mechanical properties are very low and the rate of strengthening in the precipitation reaction is very slow compared with alloys of lower r values [10]. Thus, to be able to handle the cast battery grids from Pb–Ca–Sn alloys, manufacturers have tended to produced both flat-plate and tubular grids from alloys with r values below 9:1. The large spines of tubular grids are difficult to handle if the cast alloy is mechanically very weak (approaching pure lead) when initially cast. In addition, these alloys may take weeks to age harden to acceptable levels, instead of hours or days for low r value alloys.

Low r value materials have, in general, led to poor performance of tubular grids produced for VRLA batteries. Insufficient tin has given rise to PCL which, in turn, has limited the capacity of tubular VRLA batteries. The high corrosion rates shown in Table 3 for alloys above about 0.07 wt.% Ca indicate the detrimental effects of not only Pb_3Ca precipitation above the peritectic point, but also the effects of low r values.

It is believed that creep of the positive grid alloy provides a significant acceleration of the corrosion process. Large-grained materials produced from high r values are significantly more creep resistant than low r value alloys. Low r value tubular grids suffer growth, loss of active-material adhesion, and poor rechargeability. The corrosion processes at the grid/active-material interface in low creep-resistant material may also contribute to the problem.

Table 2
Mechanical properties and corrosion of binary lead–calcium alloys

Calcium content (wt.%)	Yield strength (MPa)	Tensile strength (MPa)	Ratio YS/UTS	Creep to failure at		Corrosion rate (mm/yr)
				20.7 MPa (h)	13.8 MPa (h)	
0.025	17.7	25.1	0.71	1		0.279
0.050	29.0	37.2	0.78	30		0.345
0.065	31.8	42.5	0.75	50		0.348
0.075	35.3	46.4	0.78	40		0.358
0.090	32.9	47.0	0.70	20	100	0.392
0.100	32.5	47.8	0.68	10	40	0.411
0.110	30.5	46.3	0.66	7		0.429
0.120	27.6	43.2	0.64	5		0.480
0.140	24.7	39.2	0.63	2		0.513

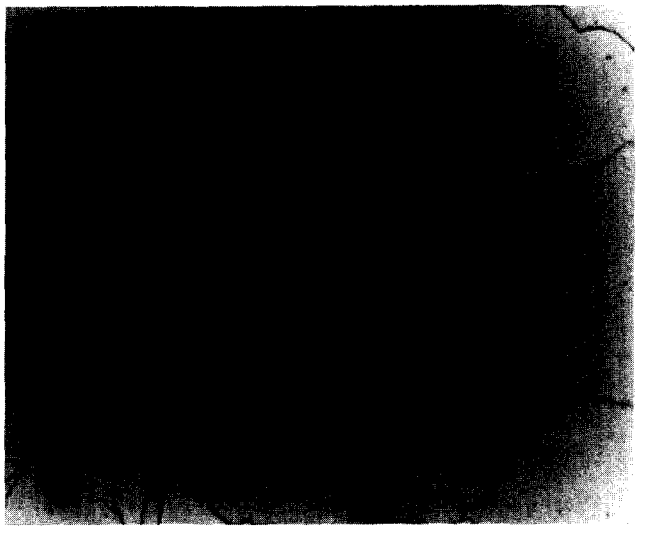

Fig. 7. Grain structure of cast Pb–0.04wt.%Ca alloy. Magnification 160×.

Fig. 8. Grain structure of cast Pb–0.10wt.%Ca alloy. Magnification 100×.

Fig. 11 gives the corrosion at the grid/active-material interface of a tubular VRLA battery spine that has suffered premature capacity loss and active-material shedding. The corrosion product on the surface of the spine is thick and exhibits the characteristic cracks parallel to the surface of the grid that lead to poor capacity. In addition, the corrosion product has separated from the grid surface in some places. The high corrosion rate and cracking of the corrosion product are believed to be due to the poor mechanical properties (particularly creep) of the alloy. The alloy contains 0.09 wt.% Ca and 0.3 wt.% Sn (i.e., an r value of 3:1) and will give a creep rate (SR hours) of about 30 h at 20.7 MPa. This is more than an order of magnitude lower than the highest creep-resistant Pb–Ca–Sn alloys and three orders of magnitude lower than high antimony alloys.

Fig. 11 also shows significant deformation of the grid material ahead of the corrosion product where it has penetrated into the grid surface. Significantly, the deformation has produced cracks that run parallel with the grid surface. These cracks, once penetrated by the electrolyte, can produce significant corrosion beneath the grid surface. The corrosion product, in layers parallel to the surface, may contribute to the formation of the poorly adhering corrosion layers in Pb–Ca–Sn alloys.

High mechanical properties, particularly creep resistance, may decrease the tendency of the grid corrosion product to deform the grid surface and produce detrimental adherence between grid and active material. Table 3 also shows the results of silver addition to Pb–Ca–Sn alloys. This increases significantly the creep resistance of the alloys [13].

3.3. *Wrought Pb–Ca–Sn alloys*

One of the major ways to increase the mechanical properties of Pb–Ca–Sn alloys is to roll the material. Table 4 shows the mechanical properties of rolled Pb–Ca–Sn alloys with variations in calcium and tin

Table 3
Mechanical properties and corrosion of cast lead–calcium–tin alloys

Calcium content (wt.%)	Yield strength (MPa)	UTS (MPa)	Yield strength (MPa)	UTS (MPa)	Creep to failure at 20.7 MPa (h)		Corrosion (mm/year)	
	0.5 wt.% Sn		1.5 wt.% Sn		0.5 wt.% Sn	1.5 wt.% Sn	0.5 wt.% Sn	1.5 wt.% Sn
0.025	19.3	25.5	34.3	45.8	10	30	0.256	0.246
0.050	38.5	48.2	46.8	55.1	70	100	0.310	0.271
0.065	40.0	48.9	49.1	58.6	200	750	0.317	0.289
0.075	40.2	50.3	49.2	60.1	300	1000	0.325	0.297
					2000 at 13.8 MPa			
0.090	40.0	51.3	46.9	58.6	100	600	0.320	0.307
0.100	38.7	51.7	43.7	57.9	70	250	0.343	0.345
					280 at 13.8 MPa			
0.120	31.1	45.8	41.7	57.2	20	140	0.365	0.345
0.140	31.2	46.5	39.5	56.5	15	120	0.368	0.337
0.080+0.2Ag		62.7			>17600 at 13.8 MPa			

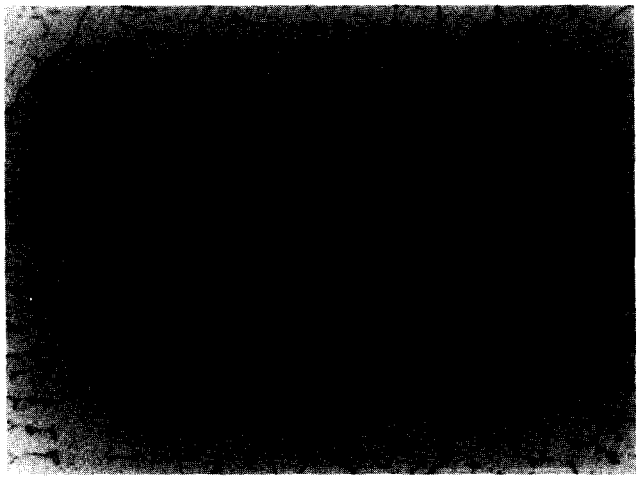

Fig. 9. Grain structure of Pb–0.07wt.%Ca–1.5wt.%Sn. Magnification 160×.

Fig. 10. Grain structure of cast Pb–0.10wt.%Ca–1.0wt.%Sn alloy. Magnification 160×.

Fig. 11. Corrosion layer on tubular Pb–0.09wt.%Ca–0.3wt.%Sn alloy grid. Magnification 160×.

contents. All the materials have been rolled with a reduction ratio of about 10:1. The alloy compositions have also been restricted to alloys below the peritectic composition.

As seen in Table 4, rolling increases the mechanical properties of all the alloys. In addition, rolling increases significantly not only the UTS and YS, but also decreases markedly the elongation and increases the stress rupture life. The alloys in Table 4 have been tested at 27.6 MPa instead of the lower stress level of 20.7 M/d for the cast Pb–Ca and Pb–Ca–Sn alloys of Tables 2 and 3. The higher stress levels permits the tests to be performed in shorter times and can be extrapolated to lower stress levels.

The highest mechanical properties are achieved at each calcium content at tin levels about 2.0 wt.%. The high tin levels may also prove to be beneficial in imparting improved conductivity to the corrosion layer.

Table 4
Mechanical properties of wrought lead–calcium–tin alloys

Calcium content (wt.%)	Tin content (wt.%)	Yield strength (MPa)	Tensile strength (MPa)	Ratio YS/UTS	Elongation (%)	Creep to failure at 27.6 MPa (h)
0.025	0.5	31.1	40.0	0.78	30	10
	1.0	47.5	57.9	0.82	20	20
	1.5	50.2	58.6	0.86	20	30
	2.5	41.8	51.7	0.80	20	10
0.050	0.5	45.3	55.2	0.82	30	10
	1.0	52.8	61.4	0.86	25	150
	1.5	57.4	63.8	0.90	15	300
	2.5	61.3	68.9	0.89	15	400
0.070	0.5	45.0	62.1	0.70	30	20
	1.0	64.0	68.9	0.93	15	400
	1.5	65.3	71.0	0.92	14	1000
	2.0	68.9	74.4	0.93	12	(8000) at 20.7 MPa (>20000) at 13.8 MPa
(+0.05 Ag)	2.0	76.8	80.0	0.96	10	(>2000)
0.080	0.5	29.6	41.4	0.71	35	8
	1.0	52.8	58.7	0.90	25	250
	1.5	66.0	71.8	0.92	20	600
	2.0	69.3	73.7	0.94	20	850 (extrapolated values)

It is interesting to note that the wrought Pb–Ca–Sn alloys with high tin content have mechanical properties similar to those of the cast high-antimony alloys. The YS of the high strength wrought Pb–Ca–Sn alloys also reaches a high ratio of the ultimate tensile strength. This means that the material can accommodate much more stress before deforming than similar composition cast alloys. Less deformation should mean better adhesion between the grid and the active material.

Fig. 12 shows the grain structure of a rolled Pb–Ca–Sn alloy containing 0.07 wt.% calcium and 1.3 wt.% tin. This structure shows orientation in the rolling direction.

Fig. 12. Grain structure of rolled Pb–0.07wt.%Ca–1.3wt.%Sn alloy. Magnification 320×.

Fig. 13. Grain structure of rolled Pb–0.07wt.%Ca–1.3wt.%Sn alloy at high magnification. Magnification 2000×.

At high magnification (Fig. 13), the orientation of fine precipitate particles of $Pb(Sn,Ca)_3$ is seen within the rolled grains. This orientation is not dissimilar to the orientation of the antimony particles shown in Fig. 1. Silver enhances the mechanical properties of the wrought Pb–Ca–Sn alloys, as seen in Table 4.

3.4. Wrought tubular grids

The major problem in the conversion of the rolled material to battery grids has been in the processing. Automotive batteries utilize expanded mesh from both

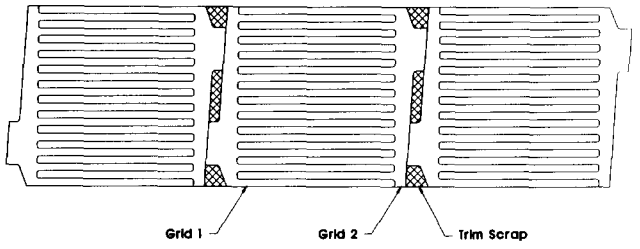

Fig. 14. Configuration for continuously cut spine grids from rolled lead strip.

cast and wrought materials for grid production. In the production of the grid, metal is significantly disturbed at the nodes during the expansion process. This can lead to a reduction in mechanical properties.

Tubular grids offer a unique way to utilize the outstanding mechanical properties of wrought strip materials with automated production techniques. Fig. 14 shows a method to cut the tubular grids from wrought sheet using either a punch or a rotary cutter. Only about 3.5% of the material is lost in the production process.

4. Conclusions

The wrought design offers an improved grid/active-material surface area compared with conventional tubular grids. The mechanical properties of the wrought material are higher in the longitudinal direction than in the transverse. This results in improved resistance to growth. The increased surface area should lead to improved high-rate discharge capacity as well as recharge capability.

Wrought tubular grids are fully dense and have no holes or porosity that is seen in conventionally cast tubular grids. There are no cracks, incomplete fill, or brittle spines despite the high mechanical properties of the wrought material. If a spine becomes distorted, it can be bent back to the desired configuration without damage.

Wrought tubular grids for VRLA batteries produced from high strength, high tin content Pb–Ca–Sn alloys should be able to be utilized in both gel and AGM constructions. Once production techniques are developed, batteries using wrought tubular grids should be an improvement over conventional cast Pb–Ca–Sn alloy tubular grids.

References

[1] M. Barak, *Pb-62*, Lead Development Association, London, 1962, p. 107.
[2] E. Sundberg, *Pb-65*, Lead Development Association, London, 1965, p. 227.
[3] H. Borchers and W. Scharfenberger, *Metall., 20* (1966) 811.
[4] A.M. Howard and E. Willingantz, *Electrochem. Technol., 6* (1968) 370.
[5] H.E. Haring and U.B. Thomas, *Trans. Electrochem. Soc., 68* (1935) 293.
[6] H. Borchers, W. Sharfenberger and S. Henkel, *Z. Metallkd., 66* (1975) 111.
[7] R.D. Prengaman, *Fall Meet. Electrochemical Society, Las Vegas, NV, Oct. 1976.*
[8] L. Bouirden, J.P. Hilger and J. Hertz, *J. Power Sources, 33* (1991) 27.
[9] M.V. Rose and J.A. Young, *Pb-74*, Lead Development Association, London, 1974, p. 37.
[10] R.D. Prengaman, *Pb-80*, Lead Development Association, London, 1980, p. 34.
[11] J. Hertz, C. Fornasieri, J.P. Hilger and M. Notin, *Proc. Labat 93, Jarna, Bulgaria, 1993,* p. 42.
[12] H.K. Geiss, in *Advances in Lead Acid Batteries,* The Electrochemical Society, Pennington, NJ, 1984, p. 241.
[13] N.E. Bagshaw, *Power Sources 12,* International Power Sources Committee, Leatherhead, UK, p. 113.